Research Square

Preprints are preliminary reports that have not undergone peer review.
They should not be considered conclusive, used to inform clinical practice,
or referenced by the media as validated information.

High-yielding syntheses, crystal structures and Hirshfeld surface analysis of bis-1,1'-(2-nitropropenes) extended with benzene-1,4-diyl and biphenyl-4,4'-diyl spacers

Kostiantyn V. Domasevitch

dk@univ.kiev.ua

Taras Shevchenko National University of Kyiv

Ganna A. Senchyk

Taras Shevchenko National University of Kyiv

Harald Krautscheid

Leipzig University

Research Article

Keywords: Nitropropenes, Lone pair-π-hole interactions, Nitro group, Weak hydrogen bond, Hirshfeld surface analysis

Posted Date: August 21st, 2024

DOI: https://doi.org/10.21203/rs.3.rs-4789004/v1

License: This work is licensed under a Creative Commons Attribution 4.0 International License.
Read Full License

Additional Declarations: No competing interests reported.

Version of Record: A version of this preprint was published at Journal of Chemical Crystallography on October 11th, 2024. See the published version at https://doi.org/10.1007/s10870-024-01032-3.

High-yielding syntheses, crystal structures and Hirshfeld surface analysis of bis-1,1′-(2-nitropropenes) extended with benzene-1,4-diyl and biphenyl-4,4′-diyl spacers

Kostiantyn V. Domasevitch,[1] Ganna A. Senchyk,[1] Harald Krautscheid[2]

[1] Inorganic Chemistry Dpt, Taras Shevchenko National University of Kyiv, Volodymyrska Str. 64/13, Kyiv 01601, Ukraine. E-mail: dk@univ.kiev.ua

[2] Institute of Inorganic Chemistry, Leipzig University, Johannisallee 29, D-04103 Leipzig, Germany

Corresponding author:
Kostiantyn V. Domasevitch
E-mail: dk@univ.kiev.ua
orcid.org/0000-0002-8733-4630

Abstract

Crystal structures of two 2-nitropropene derivatives, namely 1,4-bis((*E*)-2-nitroprop-1-enyl)benzene and 4,4′-bis((*E*)-2-nitroprop-1-enyl)biphenyl, support relevance of lone pair-π-hole interactions of nitro groups to the crystal packing of extended polyaromatic molecules. For the former structure, these bonds complement slipped π-π interactions of the benzene rings within a basic supramolecular motif representing infinite stacks. In the biphenyl derivative, only one out of two nitro groups afford $NO_2\cdots NO_2$ bonds (N···O = 3.191(2) Å) as a local pattern. The decreased significance of lone pair-π-hole interactions is in line with growing contribution of weak dispersion forces, which favor close alignment of the molecules and larger interaction ares to generate multiple C-H···π bonds. Different types of C-H···O, C-H···π, π-π, NO_2-π, $NO_2\cdots NO_2$, tetrel $CH_3\cdots O$ and $CH_3\cdots\pi$ bonds, which actualize in the prefesent structures were further assessed by Hirshfeld surface analysis and intermolecular interaction energies were calculated using the CE B3LYP/6 31G(d,p) energy model. In addition, the facile and high-yielding preparations by condensation of dialdehydes and nitroethane, provide a straightforward access to the present 2-nitropropenes, as valuable synthetic intermediates.

Keywords

Nitropropenes · Lone pair-π-hole interactions · Nitro group · Weak hydrogen bond · Hirshfeld surface analysis

Introduction

Different kinds of supramolecular bonding with nitro groups represent particular paradigms for solid-state chemistry of materials. A diversity of the interaction patterns and structural functions of NO_2 groups originates in their dual nature providing combination of negatively polarized atoms and π-hole sites [1]. In this regard, the nitro groups are self-complementary and this feature is best reflected by a possibility for direct $NO_2\cdots NO_2$ bonding involving two groups as donor and acceptor [2]. Such mutual lone pair-π-hole interactions are essentially attractive with the usual interaction energies of -10-13 kJ/mol [3], although much larger values up to -33.6 kJ/mol are also possible [4]. These parameters are comparable to commonly observed weak C-H···O bonding, but structural significance of $NO_2\cdots NO_2$ interactions may be even higher for the substrates bearing multiple nitro functionalities. For example, such bonds are primarily responsible for the generation of trigonal non-covalent nets in hexakis(4-nitrophenyl)benzene [5], for the concerted polar molecular alignment in 3,5,7-trinitro-1-azaadamantane [6] and for the packing patterns of energetic material 3,3′,5,5′-tetranitro-4,4′-bipyrazole [7].

In this view the $NO_2\cdots NO_2$ interactions could be highly relevant to developing polynitro energeric materials since the close situation of explosophores is essential for intermolecular vibrational energy transfers [8] and relaxation [9]. π–Hole interactions of nitro groups are found for both polymorphs of TNT [10]. This case and many other types of polynitro energetic systems imply the nitro groups installed at the aromatic platforms, and therefore the mutual NO_2/NO_2 bonding may face the competition not only with C-H···O hydrogen bonds, but also with the rival $NO_2\cdots\pi$ and π-π interactions. Combination of such parallel interactions with the nitro groups is itself applicable for induction of π-π stackings [11] and this may result in the generation of layered morphologies. The latters are beneficial for designing structures of insensitive explosives due to the ability of layered patterns to buffer against external mechanical stimuli [12]. In the present work, the interplay of $NO_2\cdots NO_2$, NO_2-π, π-π, C-H···O and tetrel $CH_3\cdots O$ bonding was examined for bifunctional 2-nitropropen-1-yl systems. Recently, we have shown that the non-covalent framework of parent 2,5-dinitro-2,4-hexadiene, which is a simple 2-nitropropen-1-yl duo, is dominated by lone pair-π-hole interactions [13]. At the same time, with incorporation of aromatic spacers of variable lengths, *e.g.* 1,4-phenylene or 4,4′-biphenylene in 1,4-bis((*E*)-2-nitroprop-1-enyl)benzene (**1**) or 4,4′-bis((*E*)-2-nitroprop-1-enyl)biphenyl (**2**), respectively (Scheme 1), a more complicated behavior could be anticipated as a result of coexistence of the above interaction pathways. 2-Nitropropen-1-yls receive attention also as valuable intermediates

for the syntheses of amphetamine series, substrates for Michael reactions and dipolar cycloadditions.

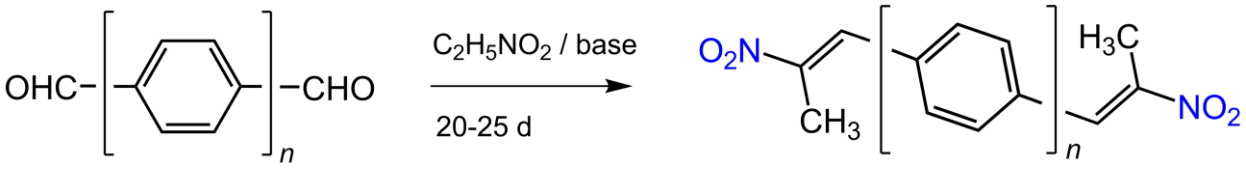

1: n = 1; 77%

2: n = 2; 81%

Scheme 1 Synthesis and molecular structures of **1** and **2**

Experimental

Synthesis of 1

40.00 g (0.30 mol) of solid terephthaldialdehyde was added to a mixture of nitroethane (113 ml, 1.57 mol) and 2-propanol (60 ml) followed by addition of 1.2 ml (18 mmol) of dry 1,2-diaminoethane. The suspension was stirred for 2 d until total dissolution of starting material and then the obtained clear yellow solution was stored in a stoppered flask at 30-35ºC. Large orange crystals of the product deposited after 18-20 d, and after the next 5 d they were filtered and washed with two 50 ml portions of cold 2-propanol (yield: 56.91 g, 77%). Pure orange crystalline material was obtained after recrystallization from 2-propanol with a 90% recovery.

Anal. Calcd for $C_{12}H_{12}N_2O_4$: C, 58.06; H, 4.87; N, 11.29. Found: C, 58.44; H, 4.82; N, 10.96.

^{1}H NMR (400 MHz, DMSO-d_6, 25ºC): δ = 8.10 (s, 2H), 7.70 (s, 4H), 2.41 (s, 6H) ppm.

^{13}C NMR (126 MHz, DMSO-d_6, 25ºC): δ = 149.0, 134.0, 132.6, 131.1, 14.4 ppm.

IR (KBr, cm^{-1}): 522 m, 543 s, 685 w, 721 m, 787 m, 842 s, 868 m, 922 s, 970 w, 983 s, 1095 w, 1127 w, 1215 m, 1289 s, 1323 vs, 1351 w, 1386 m, 1416 m, 1442 m, 1498 vs, 1523 vs, 1654 s, 2813 w, 2976 w, 3062 w.

Melting point (2-propanol) = 123-124 ºC.

Synthesis of 2

30.00 g (0.14 mol) of solid biphenyl-4,4′-dicarbaldehyde was added to a mixture of nitroethane (56 ml, 0.78 mol) and 2-propanol (70 ml) followed by addition of 1.0 ml (15 mmol) of dry 1,2-diaminoethane. The reaction mixture develops light-yellow color immediately. It was stored in a stoppered flask and stirred for 14 d at 30-35°C. After the first 4 d, total dissolution of the dicarbaldehyde was observed and then the obtained clear yellow solution slowly deposited the reaction product during next 10 d of stirring. The precipitate was filtered and thoroughly washed with two 20 ml portions of 2-propanol. The yield was 37.46 g (81%). Pure light-orange crystalline material was obtained after recrystallization from 1,4-dioxane with a 75% recovery.

Anal. Calcd for $C_{18}H_{16}N_2O_4$: C, 66.65; H, 4.97; N, 8.64. Found: C, 66.39; H, 5.07; N, 8.27.

^{1}H NMR (400 MHz, DMSO-d_6, 25°C): δ = 8.11 (s, 2H), 7.86 (d, *J* = 8.0 Hz, 4H), 7.68 (d, *J* = 8.0 Hz, 4H), 2.44 (s, 6H) ppm.

^{13}C NMR (126 MHz, DMSO-d_6, 25°C): δ = 148.1, 140.7, 133.1, 132.2, 131.6, 127.5, 14.4 ppm.

IR (KBr, cm^{-1}): 520 m, 541 m, 562 w, 708 w, 729 w, 820 s, 841 w, 870 s, 920 s, 979 s, 1004 m, 1096 w, 1133 w, 1188 m, 1217 m, 1291 m, 1317 vs, 1351 m, 1388 m, 1402 w, 1438 m, 1506 vs, 1525 m, 1604 s, 1646 m, 2810 w, 2923 w, 3060 w.

Melting point (1,4-dioxane) = 174-175 °C.

Crystallography

The diffraction data were collected with graphite-monochromated Mo Kα radiation (λ = 0.71073 Å) using a Stoe IPDS-2T diffractometer (φ oscillation scans). The structures were solved by direct methods and refined by full-matrix least-squares on F^2 using the SHELXS-97 and SHELXL-2019/3 programs [14, 15]. All hydrogen atoms were located and then freely refined with isotropic displacement parameters. Graphical visualization of the structures was made using the program Diamond [16]. Structural and refinement parameters are given in Table 1. Bond lengths, angles and atomic displacement parameters are given in the supplementary information.

Results and Discussion

Synthesis and spectral properties

The bis-nitropropenyl compounds were successfully synthesised by nitroaldol condensation (Henry reaction) starting with appropriate dialdehydes. Albeit this methodology was applicable

Table 1 Summary of crystallographic data obtained for compounds **1** and **2**

	1	**2**
CCDC deposition numbers	2372871	2372872
Formula	$C_{12}H_{12}N_2O_4$	$C_{18}H_{16}N_2O_4$
M	248.24	324.33
T/ K	173	173
Crystal system	Monoclinic	Orthorhombic
Space group, *Z*	$P2_1/n$, 2	*Pbca*, 8
a/ Å	3.8841(6)	7.4401(8)
b/ Å	9.6332(11)	19.5621(19)
c/ Å	15.8135(18)	21.865(2)
α/ º	90	90
β/ º	91.333(12)	90
γ/ º	90	90
V/ Å^3	591.52(13)	3182.3(6)
μ(Mo-Kα)/ mm^{-1}	0.106	0.097
D_{calc}/ g cm^{-3}	1.394	1.354
θ_{max}/ º	29.48	27.10
Measd/ Unique / Observed reflns.	4240/ 1638/ 1294	11563/ 3507/ 1453
Dataset completeness/ %	995	997
R_{int}	0.0141	0.0570
Parameters refined	106	281
$R1$ ($I > 2\sigma(I)$), w$R2$ (all data)	0.0446, 0.1183	0.0346, 0.0617
Goof on F^2	1.066	0.773
Max, min peak/ e Å^{-3}	0.19, -0.24	0.11, -0.13

to a vast variety of nitrostyrene derivatives, examples for the efficient high-yielding syntheses of polyfunctional alkylnitrostyrenes are relatively scarce. This may be attributed to formation of mixtures, while larger excess of the nitroethane substrate favors the subsequent Michael addition. Nature of base catalyst is also important, since 1,4-bis((*E*)-2-nitroprop-1-enyl)benzene was previously prepared in low yield in the presence of triethylamine, but with primary amines the reaction failed [17]. When reacted in a sealed tube, terephthaldialdehyde and nitroethane afforded the target product in 47% yield [18]. We suggest very simple precedures involving 6-10

mol % ethylenediamine catalyst in 2-propanol solution. The reaction mixtures slowly deposited almost pure insoluble products in the yields of about 80%, and these yields were nearly invariant for the batch scales of 5 mmol to 0.5 mol of the dialdehyde substrate. Longer reaction times, however, led to gradual dissolution of the products and decreased the yield in effect.

For both the compounds, the NMR spectra are indicative of trans (*E*) configuration of the nitro and aromatic groups, which is dominant for the most related systems. None of the spectra exhibited peaks associated with the presence of other isomers. In particular, the 1-propene CH absorbances at 8.10 (**1**) and 8.11 ppm (**2**) appear signicantly downfield the charactersitic range of 6.25-6.64 ppm for isomeric (*Z*)-nitropropenes, being a primary indicator for the assignment of the isomers [19]. A ^{13}C-NMR spectral attribution of the compounds is plausible on a base of relative intensities of the signals and comparative analysis of previous spectral data. Three signals of the side nitropropene linkage are less sensitive to the ring-substituent effects, being nearly the same for **1** and **2** as well as for a selection of related (2-nitroprop-1-en-1-yl)benzenes [20]. The lowest-field signals, about the similar chemical shifts of 149.0 (1) and 148.1 ppm (2), are ascribed to C-β, the C-γ are easily identified as the signals at highest field, while C-α are at 132.6 and 133.1 ppm, respectively. Higher transmission of electronic effects through vinyl bridge, as may be compared with $–C_6H_4$-CH=C(CH_3)NO_2, has certain indication rather in the C-1 shifts. Whereas C-1 for (2) at 132.2 ppm is close to 132.8 ppm for the parent (2-nitroprop-1-en-1-yl)benzene [20], this signal for **1** is detected about 2 ppm to lower field.

The FT-IR data are consistent with the expected structure. The most prominent features are very strong $\nu_s(NO_2)$ and $\nu_{as}(NO_2)$ bands, which for **1** and **2** are detected at 1323, 1523 cm^{-1} and 1317, 1506 cm^{-1}, respectively. The relatively intense bands at 1654 (**1**) and 1646 cm^{-1} (**2**) correspond ν(CC) (vinyl), while strong line at 1604 cm^{-1} for **2** is ν(CC) (ring). For **1**, the latter band is not detectable, like in the case of other symmetrical 1,4-substituted benzenes [21]. The observed trends in $\nu_s(NO_2)$ and ν(CC) (vinyl), when compare FT-IR for **1** and **2**, are in line with the fact that these frequencies of 4-R-(2-nitroprop-1-en-1-yl)benzenes correlate with Hammett parameters of the 4-substituent (4-R) on the aromatic ring [22]. A certain high frequency shift of ν(CC) for **1** supports higher degree of conjugation through short vinyl bridge (R = -CHC(CH_3)NO_2), as it was already detected by ^{13}C NMR data. In the case of direct nitro-phenylene bond (R = -NO_2) this effect is more perceptible (ν(CC) = 1661 cm^{-1}) [22].

Crystal Structures

The molecular structures of the compounds are shown in Fig. 1. For **1**, the independent part comprises half-molecules situated across centers of inversion. The primary supramolecular

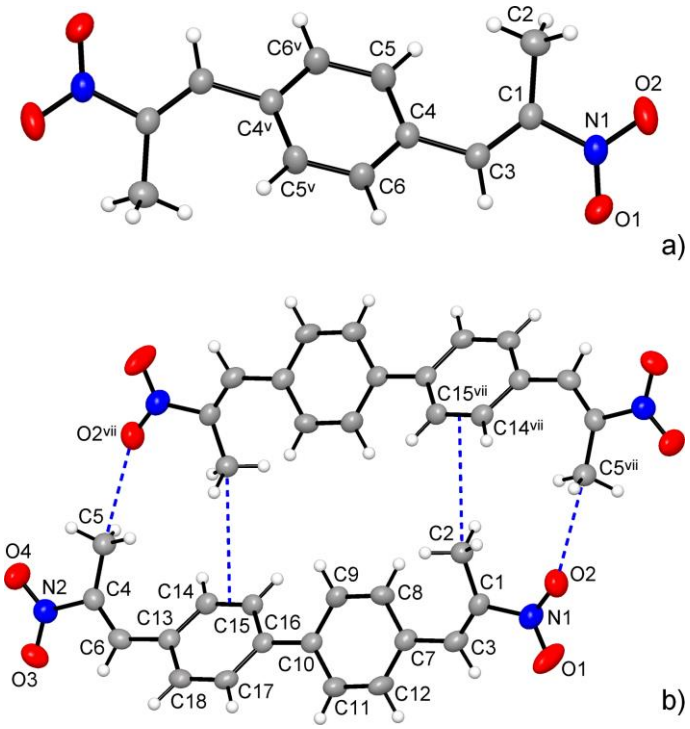

Fig 1 (a) The molecular structures of **1**, showing displacement ellipsoids drawn at the 50% probability level. (b) The molecular structure of (2) with 40% displacement ellipsoids. Second molecule completes the centrosymmetric dimer formed through two pairs of the tetrel bonds, which are indicated with dotted blue lines. Symmetry code for **1**: (v) $-x+1, -y, -z$; for **2**: (vii) $-x+1, -y+1, -z+1$.

bonding in the structure of **1** is combined slipped π-π and double lone pair-π hole $NO_2\cdots NO_2$ interactions between the translation related molecules, which arrange the latters into the 1D stacks along the crystal *a*-direction (Fig. 2). In spite of actually small and appropriate slippage angle of 16.7(2)°, the π-π stacking is weak and very distal, with the π···π separation (defined as a distance bentween the two ring centroids) of 3.884(2) Å and with shortest contact of C···C = 3.742(2) Å. As well, for the nitro-nitro stacks, $N1\cdots O1^{vi}$ [(vi) $x+1, y, z$] contacts are also as long as 3.415(2) Å. One can note that such slipped-parallel π-π stacking itself could be somewhat deficient due to the electrostatic repulsion. There is a certain electrostatic destabilization (E_{ele} = +4.1 kJ mol^{-1}) even in the case of slipped-paralell nitrobenzene dimers [23], but for 1,4-substituted benzenes with two identical acceptor groups this effect may be more appreciable thus preventing π-stacking, unless it is not compensated by other forces. For example, 1,4-dinitro- [24] and 1,4-diflurobenzenes [25] do not exhibit any aromatic π-π interactions at all, while in the case of 4,4′-dinitobiphenyl [26], similarly to the structure of **1**, the π-π stacking is made possible

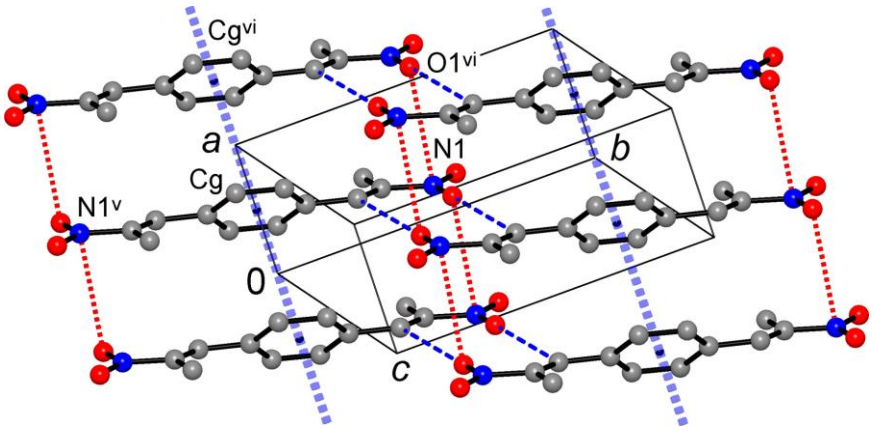

Fig 2 Basic motif of the crystal structure of **1**, with 1D stacks propagating along the *a*-direction, which involve the combinations of slipped π-π interctions (thick dotted lines) and pairs of lone pair-π-hole NO_2/NO_2 bonds (dotted red lines). Cg is the aromatic ring centroids.
Symmetry codes: (v) *–x*+1, *-y*, *-z*; (vi) *x*+1, *y*, *z*.

with a larger contribution from dispersion forces and with complementary double lone pair-π hole $NO_2\cdots NO_2$ interactions.

Very extensive weak C-H···O bonding involving every of the present O-acceptors is important for interaction between the adjacent stacks. The hydrogen-bond connectivity affords the layers, which are parallel to the (101) plane (Fig. 3), with the most directional bond established by methyl group C2-H2A···O2^{i} (C2···O2^{i} = 3.415(2) Å; C2-H2A···O2^{i} = 138.2(17)^{o}; Table 2). Assembly of the molecules into the centrosymmetric dimers through two pairs of C3-H3···O1^{iv} and C6-H6···O1^{iv} bonds (Fig. 3, Table 2) is completely inherited from the structure of the mofunctional prototype, 1-phenyl-2-nitro-1-propene [27]. Such mutual double C-H···O bonding itself may be regarded as supramolecular synthon for crystal engineering with nitropropenyl species. However, the attribution of the layers is only formal since the interlayer bonding is stronger and more directional. This favorable geometry is influenced by non-planar structure of the molecule. Due to the appreciable twist angle subtended by the ring and nitropropenyl fragments, two nitro-O acceptors are taken out of the layer plane and they are oriented towards the CH_3 and CH-donors from the previous and next layers. For example, the most polarized ethene C3-H3 donors adopt even double bonding, but the afore mentioned C3-H3···O1^{iv} bond within the layer (H3···O1^{iv} = 2.98(2) Å; C3-H3···O1^{iv} = 107.0(14)^{o}) exists as weaker and less directional branch accompanying the intelayer C3-H3···O1^{iii} bond (H3···O1^{iii} = 2.56(2) Å; C3-H3···O1^{iii} = 164.0(16)^{o}). The shortest C···O separations within the C-H···O

Table 2 Hydrogen bonding parameters (Å, °)[a)]

Compound	D-H···A	D-H	H···A	D···A	∠D-H···A
1	C2-H2*A*···O2^{i}	0.97(2)	2.63(2)	3.415(2)	138.2(17)
	C2-H2*C*···O2^{ii}	0.96(2)	2.514(19)	3.173(2)	125.9(14)
	C3-H3···O1^{iii}	0.94(2)	2.56(2)	3.475(2)	164.0(16)
	C3-H3···O1^{iv}	0.94(2)	2.98(2)	3.373(2)	107.0(14)
	C5-H5···O2^{i}	0.998(18)	2.602(18)	3.592(2)	171.4(15)
	C6-H6···O1^{iv}	0.990(19)	2.795(19)	3.588(2)	137.5(14)
2	C2-H2*B*···O1^{i}	1.016(17)	2.455(15)	3.138(3)	124.0(12)
	C2-H2*C*···O3^{ii}	0.976(17)	2.667(16)	3.601(2)	160.4(12)
	C5-H5*A*···O2^{iii}	0.972(15)	2.755(14)	3.183(2)	107.3(10)
	C6-H6···O3^{iv}	0.941(13)	2.689(13)	3.166(2)	112.1(10)
	C9-H9···O3^{v}	0.986(12)	2.603(13)	3.275(2)	125.5(10)
	C12-H12···O4^{vi}	0.976(14)	2.667(15)	3.613(2)	163.5(12)
	C14-H14···Cg2^{x}	0.943(12)	2.842(13)	3.4361(16)	121.9(12)
	C17-H17···O1^{vii}	0.969(13)	2.434(14)	3.257(2)	142.4(11)

[a)] Cg2 is centroid of the C13-C18 ring; Symmetry codes for **1**: (i) −*x*+½, *y*−½, −*z*+½; (ii) −*x*+1½, *y*−½, −*z*+½; (iii) −*x*, −*y*+1, −*z*; (iv) −*x*+1, −*y*+1, −*z*; for **2**: (i) *x*+½, *y*, −*z*+½; (ii) *x*+½, −*y*+½, −*z*+1; (iii) −*x*+1, −*y*+1, −*z*+1; (iv) −*x*+1, −*y*, −*z*+1; (v) −*x*+½, *y*+½, *z*; (vi) *x*, −*y*+½, *z*−½; (vii) −*x*+1, *y*−½, −*z*+½; (x) *x*-½, -*y*+½, -*z*+1.

bonding framework (C2···O2^{ii} = 3.173(2) Å; Table 2) are also found between the layers.

In the case of **2**, the packing is appreciably different and it involves additional kinds of interactions. A very salient feature of the pattern concerns close mutual alignment of two inversion related molecules (symmetry code (vii) –*x*+1, -*y*+1, -*z*+1), which establish two pairs of short contacts with CH_3 groups (Fig. 1). Such interactions are usually regarded as tetrel bonds [28]. In particular, the short contacts C5···O2^{vii} = 3.183(2) Å are associated with the nearly straight angles C4-C5···O2^{vii} = 161.93(14)^{o} and three C5-H···O2^{vii} angles in the range of 76.6(9)-107.3(10)^{o}. The latters are inappropriate for hydrogen bonding, while reflecting highly directional tetrel CH_3···O interaction [29]. In similar way, the second CH_3 group is functional as Lewis base for the tetrel CH_3···π bond with C2···Cg1^{vii} = 3.694(2) Å and ∠C1-C2···Cg1^{vii} = 162.2(2)^{o} (Cg1 is a centroid of the C14-C15 bond). Combination of four such interactions

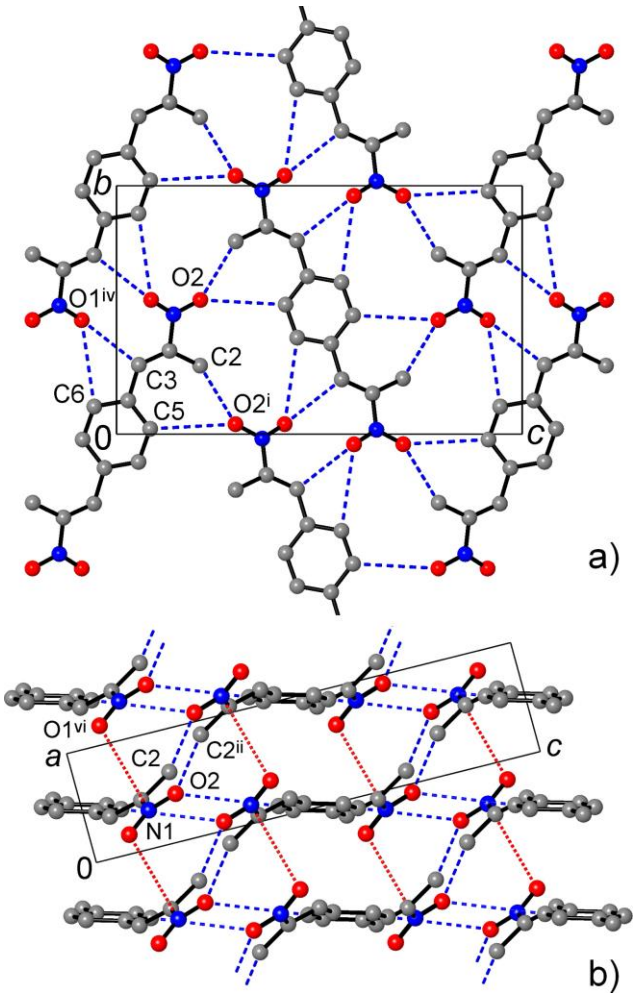

Fig 3 (a) Projection of the structure of **1** on the *bc*-plane, with the main network of weak hydrogen bonds C-H···O. (b) A side-view of three successive layers, in a projection on the *ac*-plane, showing how the inclined orientation of the nitropenyl groups facilitates the interalyer bonding.

conditiones slightly unusual molecular conformation.

When consider these peculiar dimers as structral units, a typical herringbone packing may be derived (Fig. 4). A layer of C-H···O bonded molecules propagates parallel to the *bc* plane. The most remarkable interaction is mutual ethene/nitro bonding C6-H···O3^{iii} (C6···O3^{iii} = 3.166(2) Å, Table 2), which is similar to the structure of **1**. Two directional bonds with aromatic donors, namelly C12-H···O4^{v} and C17-H···O1^{vi} (C···O are 3.613(2) and 3.257(2) Å, respectively) are also important. However, the attribution of the C-H···O bonded morphological layers in the present case is even a more nominal than for the π-π bond dominated structure of **1**. The primary bonding in **2** originates in combination of lone pair-π interactions, nitro/π stacking and multiple

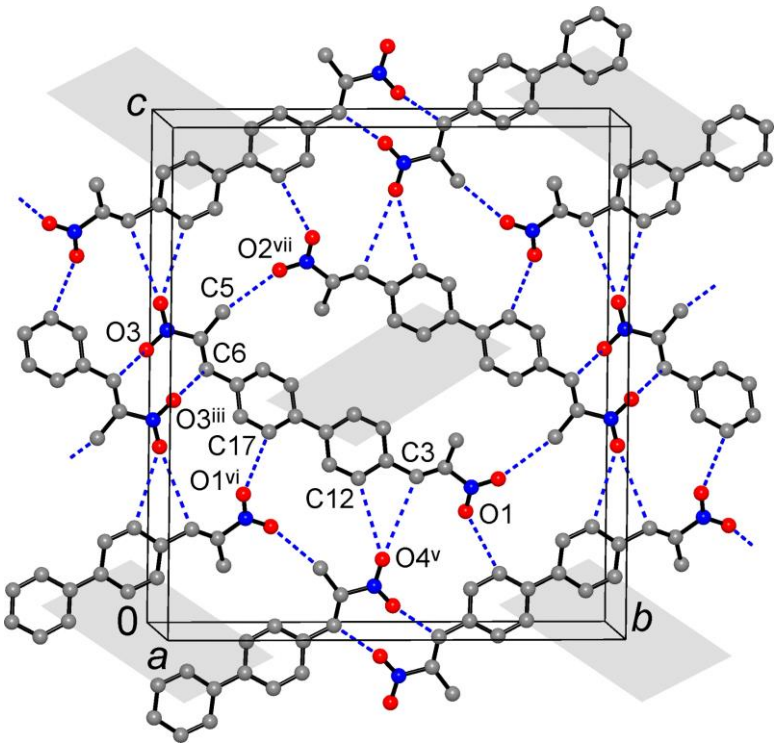

Fig 4 Projection of the structure **2** nearly on the *bc*-plane, showing the network of weak hydrogen bonds C-H···O. Grey quadrangles mark the tetrel-bond linked dimers and help to identify a typical herringbone packing motif

C-H···π bonding. The strength of nitro-nitro bonding is superior to the structure of **1**, but it engages only half of the available NO_2 groups (Fig. 5). The N1···O1^{viii} distance of 3.191(2) Å (symmetry code: (viii) *x*+½, *y*, -*z*+½) falls into the range of 2.87-3.23 Å reported for dinitrodiene compounds [13]. This interaction arranges molecules into the inclined stacks, in which the stacking axes coincide with the crystal *a*-direction. The lengthy outer -$(C_6H_4)_2$(nitropropenyl) arms of two adjacent stacks (indicated with blue and red colors in Fig. 6) interdigitate generating slipped nitro-π stacking with interplanar angle between the groups (N2/C4/O3/O4) and (C7-C12)^x of 18.11(3)^o and shortest contact N2···C8^x = 3.422(2) Å (symmetry code: (x) *x*-½, -*y*+½, -*z*+1). These interactions are accompanied with C-H···π bonds (C14···Cg2^x = 3.4361(16) Å, Cg2 is centroid of the C13-C18 ring, Table 2), which are consistent with the values for identical interaction in 1-phenyl-2-nitro-1-propene (C-H···π = 3.46 Å) [27]. Distal contacts involving CH_3 groups (C5···C10^x = 3.810(3) Å) may be related to a very weak CH_3 ···π interaction or to dispersion forces. This set of versatile bonding led by lone pair-π interactions results in generation of corrugated layers, which are parallel to the *ab*-plane (Fig. 6).

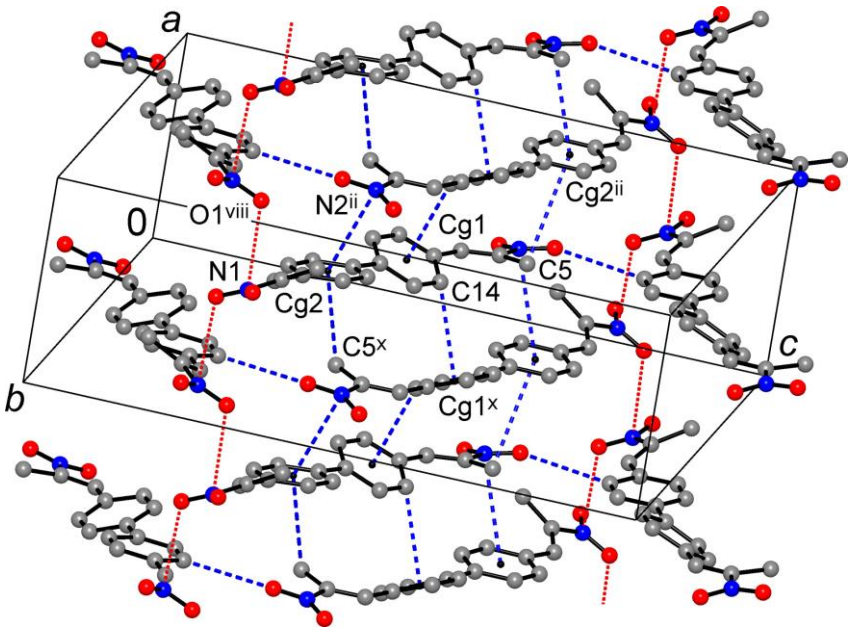

Fig 5 Two inclined $NO_2\cdots NO_2$ stacks (marked with dotted red lines) and interdigitation of their aromatic/nitropropenyl arms with the generation of multiple C-H$\cdots\pi$ and NO_2-π interactions. Cg1 and Cg2 are centroids of two aromatic rings

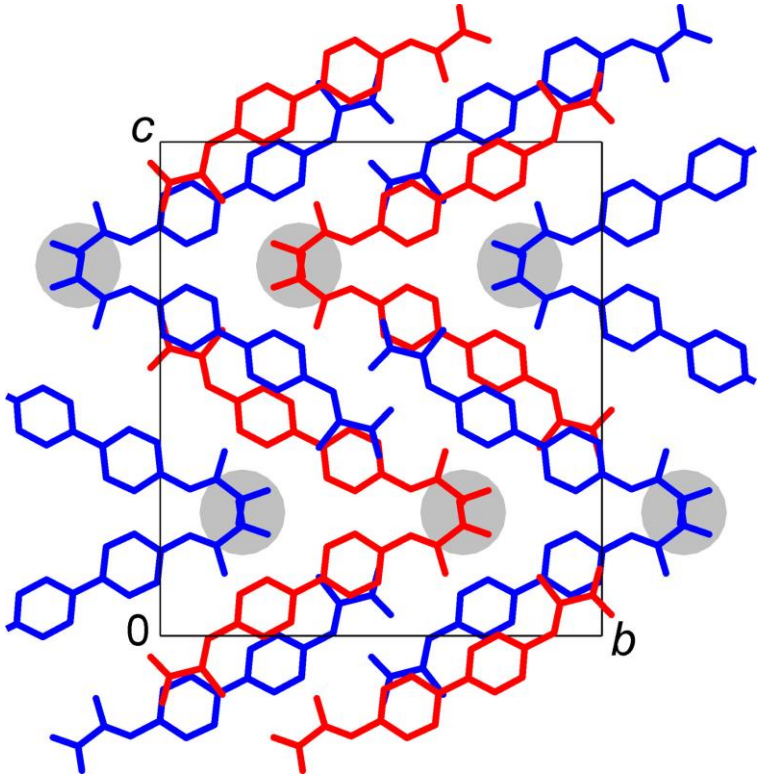

Fig 6 Packing of the $NO_2\cdots NO_2$ stacks in the structure of **2** viewed down the direction of their axes, which are orthogonal to the drawing plane and are additionally identified by a set of grey circles. The individual stacks are distinguished by red and blue colors

Hirshfeld surface analysis

The supramolecular interactions in the title structures were further assessed and visualized by Hirshfeld surface analysis [30-32] performed with CrystalExplorer17 [33]. The Hirshfeld surfaces of the molecules in **1** and **2** mapped over d_{norm} clearly indicate (red regions) a set of interaction sites (Fig. 7, 8). However, all kinds of interactions in the structures are relatively weak and intensivities even for the most prominent spots do not exceed -0.193 a.u. In the case of **1**, a few red spots (-0.053 to -0.129 a.u.) reflect weak C-H···O bonding, while π-π stacking and lone pair-π hole interactions are associated with normal van der Waals contacts (+0.042 to +0.206 a.u). In the case of **2**, the most intense spots are due to aromatic C-H···O bonding (-0.127 to -0.183 a.u.). However, even weaker methyl C-H···O and C-H···π interactions are also detectable on the surface, by several smaller diffuse spots (-0.018 to -0.068 a.u.).

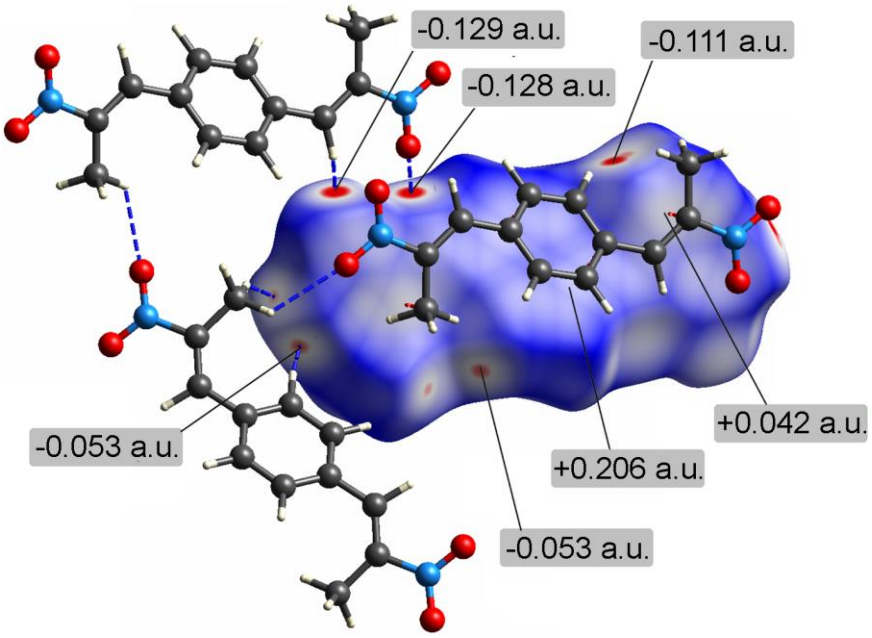

Fig 7 The Hirshfeld surface of the molecule of **1**, mapped over d_{norm} (the C-H distances are normalized) in the color range -0.13 (red) to 1.03 a.u. (blue), with the red regions indicating the donor and acceptor atoms of H···O interactions

The 2D fingerprint plots and the contributions of some types of interactomic contacts to the Hirshfeld surfaces suggest dominance of the H-atom contacts, accounting for 87.1% of the contacts in **1** and 91.8% in **2** (Fig. 9). However, the plots are clearly identifying an essential difference between two structures. A relatively compact fingerprint pattern in the case of **1** suggests a more crowded molecular environment, which is consistent with slightly higher

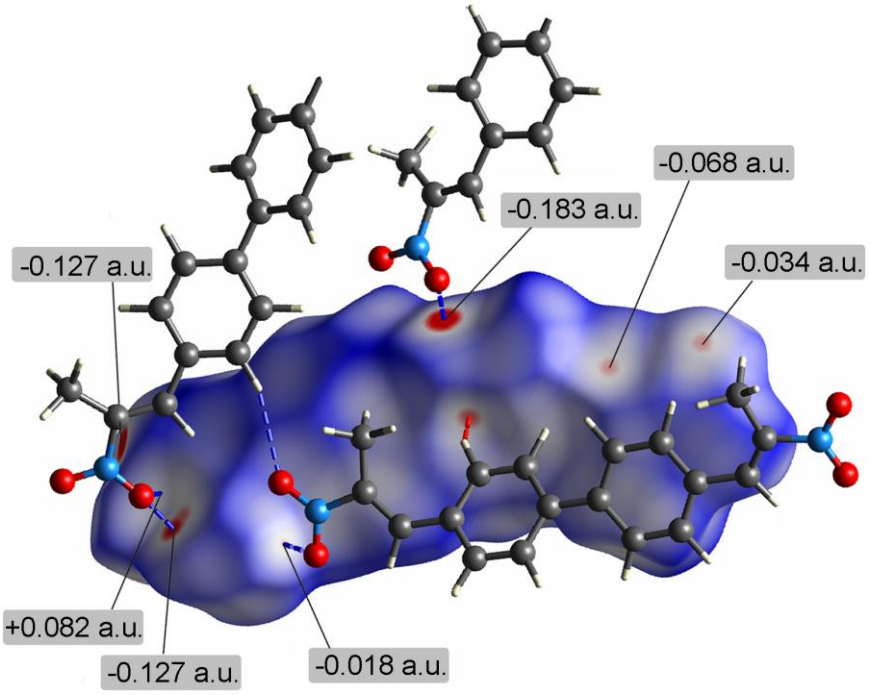

Fig 8 The Hirshfeld surface of the molecule of **2**, mapped over d_{norm} (the C-H distances are normalized) in the color range -0.19 (red) to 1.24 a.u. (blue), with the red regions indicating the donor and acceptor atoms of H···O interactions.

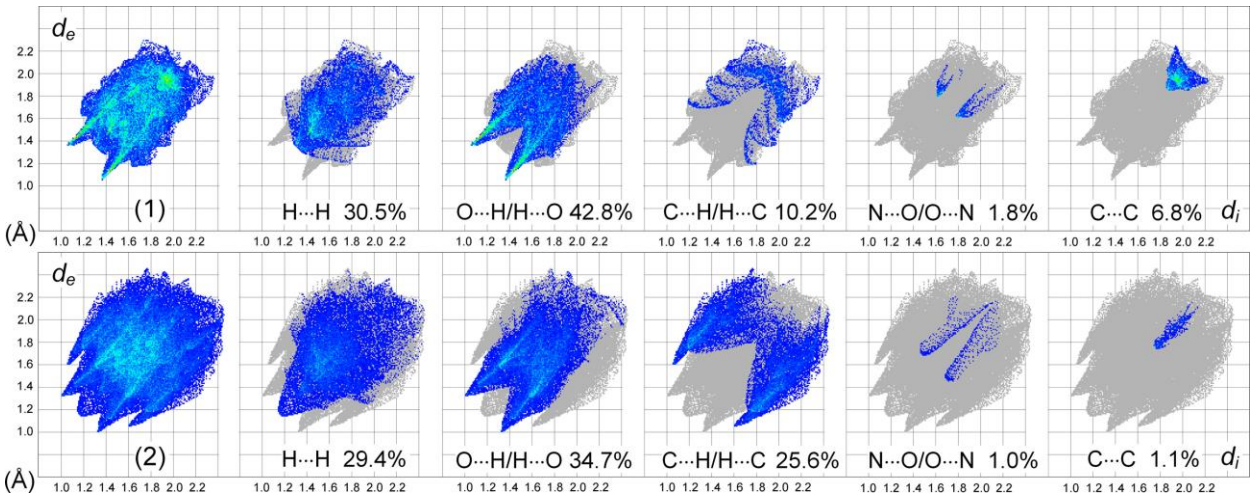

Fig 9 Two-dimensional fingerprint plots for **1** and **2**, and delineated into the principal contributions of H···H, O···H/H···O, C···H/H···C, N···O/O···N and C···C contacts. Other minor contributors (for **1** and **2**, respectively) are: O···O (2.5% and 0.9%); C···O/O···C (1.7% and 3.7%) and N···H/H···N contacts (3.6% and 2.1%).

packing index of 71.4 *versus* 70.2% for **2**. For **1**, a pair of short spikes pointing to the lower left of the plot, indicates numerous O···H/H···O interactions (42.8%), with a shortest contact of 2.45 Å. For **2** these features are also present, while fraction of O···H/H···O is contracted to 34.7%. More diffuse and broadened pattern, with a number of points at large distances, may be suggestive of a less directional bonding. In fact, some of the points correspond to CH_3···O tetrel interactions, but not to the hydrogen bonds. Thus the landscape of C-H···O bonding in the case of **2** is perceptible more scarce. Actually different packing mode is evidenced also by appearance of additional pair of shorter spikes for the C···H/H···C contacts (closest separation is 2.70 Å), which originate in C-H···π interactions and deliver 25.6% to the surface area of **2**. This feature is not detectable for **1**. The fraction of C···H/H···C contacts is still significant (10.2%), but the plots reflect them rather as a diffuse collection of the points only. Instead of the C-H···π bonds, the aromatic frames in **1** afford slipped π-π stacking. An overlap between parallel molecules is cearly reflected by the plot, in the form of blue-green area at ca. $d_e = d_i = 1.85$ Å, with contribution of C···C contacts of 6.8% (Fig. 9). The latters are much less significant (1.1 %) to the surface in **2** and suggest actually elimination of the overlap, with only one C···C contact at 3.50 Å corresponding to stacking of nitropropene and phenylene groups. Interactions of NO_2 groups are equally important for both structres, with the N···O/O···N contacts accounting for 1.8% (**1**) and 1.0% (**2**) of all contacts. For comparison, three NO_2 interaction sites of 3,5,7-trinitro-1-azaadamantane grant as much as 3.2% contacts of these relatively compact molecules [6]. With a double nitro stacking, the N···O/O···N contacts are larger in number in the case of **1**, but for **2** the only stack is denser, as it evidenced by d_e+d_i values of 3.40 and 3.20 Å, respectively.

The intermolecular interaction energies were calculated using the CE B3LYP/6 31G(d,p) energy model in CrystalExplorer17 [33]. For **1**, five symmetry-unique intermolecular paths were considered for the 14-fold closest environment of the molecule. In the case of **2**, seven unique intermolecular paths were identified. For the distinct types of intermolecular interactions in **1** (Table 3), the highest energy E_{tot} = -30.4 kJ mol^{-1} corresponds to the stack between pairs of the inversion related molecules (Type A, Fig. 10). It is comparable with value of -30.6 kJ mol^{-1} calculated for 1,3-dinitrobenzene dimer [35]. As expected for π-π interactions, the primary contributor here is London dispersion. However, a significant positive electrostatic component (E_{ele} = 10.2 kJ mol^{-1}), is rather unusual for such interactions. It originates in large Mullikan charges on C4 atoms bearing the nitropropenyl acceptors, similarly to 1-phenyl-2-nitropropene analogue [36]. One can anticipate a special importance of favorable electrostatic lone pair-π hole bonds of NO_2 groups, which beyond their contribution to the dispersion forces decrese the net

Table 3 Calculated interaction energies (kJ/mol).[a)]

Type	Symmetry code	Interaction	R	E_{ele}	E_{pol}	E_{dis}	E_{rep}	E_{tot}
Compound **1**								
A	*x*+1, *y*, *z*	π-π, NO_2···NO_2 (2×)	3.88	10.2	-3.6	-64.6	28.8	-30.4
B	-*x*, -*y*+1, -*z*	CH···O (2×)	10.39	-13.9	-2.9	-9.5	11.1	-18.2
C	-*x*+½, *y*+½, -*z*+½	CH···O (2×)	9.50	-7.8	-2.6	-10.5	9.4	-13.5
D	-*x*+1½, *y*+½, -*z*+½	CH···O	9.42	-3.7	-1.8	-9.7	7.7	-8.9
E	-*x*+1, -*y*+1, -*z*	CH···O (4×), dispersion	9.63	-16.5	-3.5	-16.7	9.8	-28.5
Compound **2**								
A	*x*+½, -*y*+½, -*z*+1	NO_2-π, CH···O, CH···π (2×)	6.40	-14.1	-4.3	-69.1	42.7	-51.9
B	*x*-½, *y*, -*z*+½	NO_2···NO_2, CH···O	8.30	-2.2	-2.6	-19.0	11.4	-13.8
C	-*x*+½, *y*-½, *z*	CH···O (2×), CH···π	9.99	-14.8	-4.2	-33.5	21.1	-34.9
D	-*x*+1, -*y*, -*z*+1	CH···O (2×)	14.17	-17.6	-4.3	-19.3	15.2	-29.1
E	*x*, -*y*+½, *z*+½	CH···O (2×)	11.59	-0.3	-1.9	-9.2	5.7	-6.2
F	-*x*+1, *y*-½, -*z*+½	CH···O	12.39	-11.7	-2.7	-10.1	11.5	-16.1
G	-*x*+1, -*y*+1, -*z*+1	tetrel CH_3···O, CH_3···π (2×)	7.11	0.6	-4.0	-33.5	18.1	-20.3
H	-*x*+1½, *y*-½, *z*	CH···π	11.18	-0.5	-0.5	-6.6	1.4	-5.9

[a)] Interaction energies were calculated employing the CE-B3LYP/6–31G(d,p) functional/basis set combination. The scale factors used to determine E_{tot} are: k_{ele} = 1.057, k_{pol} = 0.740, k_{dis} = 0.871, and k_{rep} = 0.618 [34]. For details of the interaction modes, see Fig. 10, 11; R is the distance between the centroids of the interacting molecules.

electrostatic repulsion as well. Other principal intermolecular pathways represent different kinds of weak hydrogen bonding only (Fig. 10). The energy of the above stack A is far superior to the single C-H···O hydrogen bonds of aliphatic donors and nitro acceptors (Type D, E_{tot} = -8.9 kJ mol^{-1}), while in the case of multiple interactions the differences are lesser. For example, two pairs of inversion-related C-H···O bonds according to the Type E provide the net interaction energy of E_{tot} = -28.5 kJ mol^{-1}.

A similar pairing pattern in **2** results in exactly the same interaction energy (Type D, E_{tot} = -29.1 kJ mol^{-1}; Fig. 11). However, the most appreciable energies in this structure are generally associated with the largest intermolecular contact areas (Types A, C, G) and are governed by dispersion contributors (Table 3). That is particularly the case of Type A path (E_{dis} = -69.1 kJ mol^{-1}) invloving two kinds of C-H···π bonds, nitro-π and two C-H···O bonds, which support the highest interaction energy of E_{tot} = -51.9 kJ mol^{-1}. Energetically favorable (E_{tot} = -20.3 kJ mol^{-1}) pairing of the molecules according to the Type G is also remarkable. It involves two types of tetrel bonds, namely CH_3···O and CH_3···π, and two pairs of such bonds acting in a synergy may be regarded as essential for stabilization of slightly unexpected molecular conformation. For

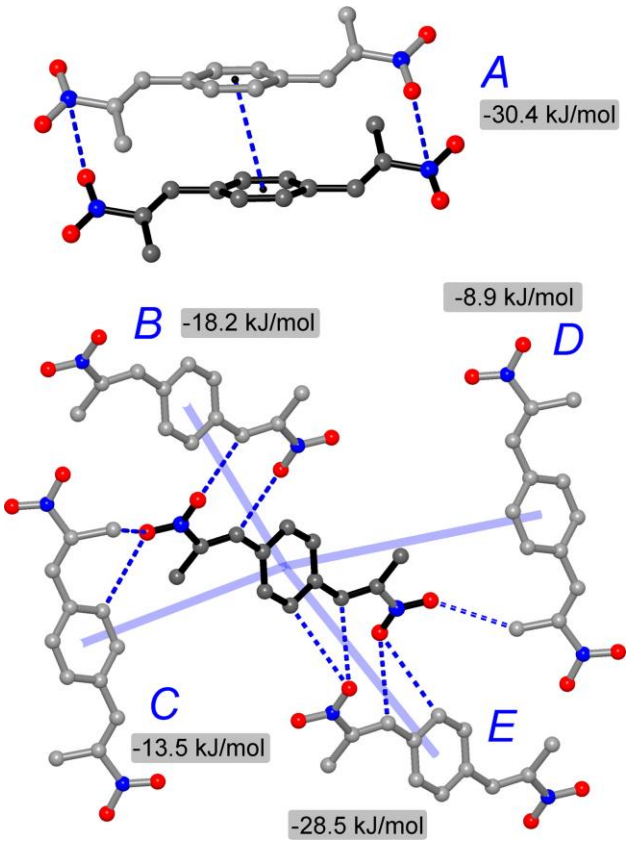

Fig 10 The five symmetry unique pathways of intermolecular interactions in **1** represented by slipped π-π and lone pair-π-hole NO_2/NO_2 interactions (A) and different modes of single (D) and multiple (B, C, E) C-H···O hydrogen bonding.

comparison, energy of single weak tetrel bond for FCH_3-ethylene complex was estimated as -5.0 kJ mol^{-1} [37]. Pairing accordingly to the Type B is due to a combination of mutual nitro-nitro and C-H···O bonds with a total interaction energy of E_{tot} = -13.8 kJ mol^{-1}. The latter is reminiscent of the energetics for comparable combination of methyl and aromatic C-H···O bonds in **1** (-13.5 mol^{-1}; Type C, Table 3). Therefore the contribution of the π–hole interaction of nitro groups may be estimated as nearly equivalent to common aromatic C-H···O bonds.

Conclusions

Structures of the examined 2-nitropropenes deliver a plethora of weak intermolecular interactions and patterns those include different kinds of C-H···O, C-H···π, π-π, NO_2-π, NO_2···NO_2, tetrel CH_3···O and CH_3···π bonds. The lone pair-π hole interactions of the nitro groups are highly competitive to the rival non-covalent bonding and they are clearly traced in both structures. However, here is a trend for the growing significance of weak dispersion forces,

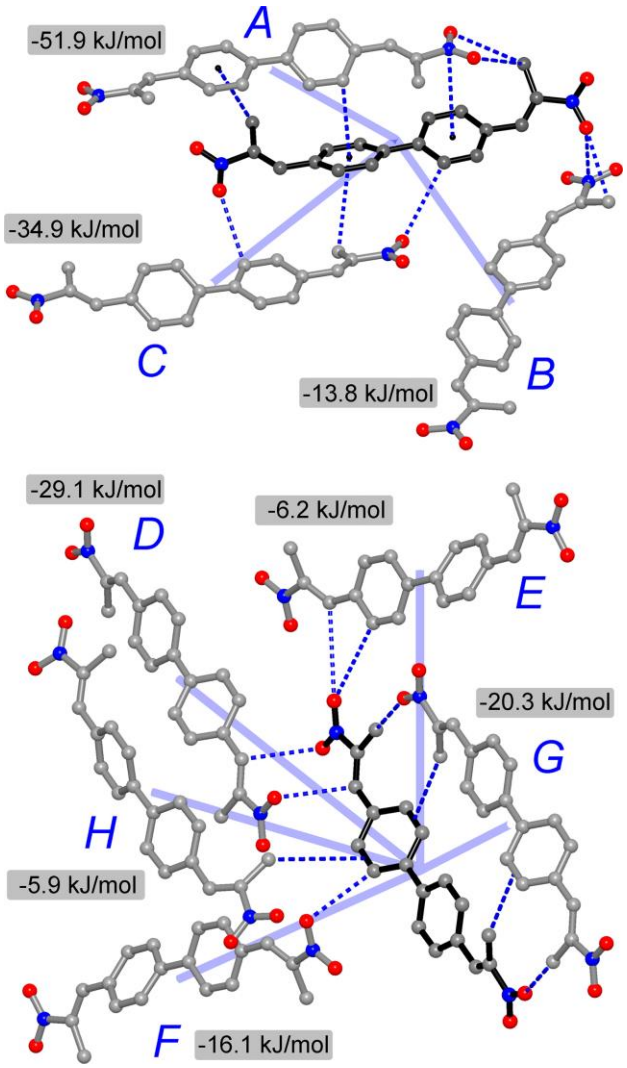

Fig 11 The principal pathways of intermolecular interactions in **2** represented by lone pair-π-hole $NO_2\cdots NO_2$ bonds (B), combination of C-H···O and C-H···π bonds (A, C), different C-H···O (D-F) and tetrel $CH_3\cdots O$ and $CH_3\cdots\pi$ bonds (G, H)

which is in line with the extension of the molecular aromatic linkage. The increase in a number of weak CH-donors for biphenyl derivative results in multiple C-H···π and tetrel $CH_3\cdots O$ and $CH_3\cdots\pi$ bonds supporting larger intermolecular interaction areas. When hidden in the shade of such weak though very extensive interactions, the nitro-nitro stacking actualizes in the form of the local pattern. At the same time, its impact for the crystal structure of phenylene derivative is still prominent for providing the primary supramolecular motif, stabilizing π-π interactions and contributing to the largest interaction energy.

Acknowledgements

The authors acknowledge the financial support from the Ministry of Education and Science of Ukraine (grant 22BF037-11) and the courage of the Armed Forces of Ukraine that made the submission of this manuscript possible.

Author Contributions K.V.D. prepared the title compounds and grew the crystals. G.A.S. performed spectral indentification, collected and refined the structures under the supervision of H.K. The authors wrote different parts of the manuscript, which was reviewed by all authors.

Data Availability The crystallographic data CIF files have been deposited at the Cambridge Crystallographic Data Centre with deposit numbers as noted in Table 1. These data can be obtained free of charge at www.ccdc. cam.ac.uk/data_request/cif, by emailing data_request@ccdc.cam.ac.uk or by contacting The Cambridge Crystallographic Data Centre, 12 Union Road, Cambridge, CB2 1EZ, UK; fax: +44 1223 336033.

Declarations

Competing interests The authors declare no competing interests.

References

[1] Bauzá A, Mooibroek TJ, Frontera A (2015) Directionality of π-holes in nitro compounds. Chem Commun 51:1491-1493. https://doi.org/10.1039/C4CC09132A

[2] Veluthaparambath RVP, Krishna V, Pancharatna PD, Saha BK (2023) Preferred geometry and nature of $NO_2\cdots NO_2$ Interactions: A statistical survey and theoretical study. Cryst Growth Des 23:442-449. https://doi.org/10.1021/acs.cgd.2c01109

[3] Bauzá A, Mooibroek TJ, Frontera A (2015) The bright future of unconventional σ/π-hole interactions. ChemPhysChem 16:2496-2517. https://doi.org/10.1002/cphc.201500314

[4] Daszkiewicz M (2013) Importance of O···N interaction between nitro groups in crystals. CrystEngComm 15:10427-10430. https://doi.org/10.1039/C3CE41788C

[5] Gagnon E, Maris T, Malyz KE, Wuest JD (2007) The potential of intermolecular N···O interactions of nitro groups in crystal engineering, as revealed by structures of hexakis(4-nitrophenyl)benzene. Tetrahedron 63:6603-6613. https://doi.org/10.1016/j.tet.2007.03.101

[6] Domasevitch KV, Senchyk GA, Krautscheid H (2020) Bulk polarity of 3,5,7-trinitro-1-azaadamantane mediated by asymmetric NO_2(lone pair)$\cdots NO_2$(π-hole) supramolecular bonding. Acta Crystallogr Sect C 76: 598-604. https://doi.org/10.1107/S2053229620006762

[7] Domasevitch KV, Krautscheid H (2024) Two metastable high hydrates of energetic material 3,3′,5,5′-tetranitro-4,4′-bipyrazole. Acta Crystallogr Sect C 80:166-176. https://doi.org/10.1107/S2053229624003346

[8] Wang R, Jiang W, Qu Z, Zhu Y, Yang Y., Wang Z. (2019) Intermolecular vibrational energy transfers in nitro-energetic molecules: A first-principles molecular dynamics study. Chem Phys Lett 733:136675. https://doi.org/10.1016/j.cplett.2019.136675

[9] Chu G, Yang Z, Xi T, Xin J, Zhao Y, He W, Shui M, Gu Y, Xiong Y, Xu T (2018) Relaxed structure of typical nitro explosives in the excited state: Observation, implication and application. Chem Phys Lett 698:200-205. https://doi.org/10.1016/j.cplett.2018.02.030

[10] Vrcelj RM, Sherwood JN, Kennedy AR, Gallagher HG, Gelbrich T (2003) Polymorphism in 2,4,6-trinitrotoluene. Cryst Growth Des 3:1027-1032. https://doi.org/10.1021/cg0340704.

[11] Sears WA, MacKinnon CD, Mawhinney RC, Sinnemaki LC, Johnson MJ, Winter AJ, Robertson CM (2010). Using the nitro group to induce π-stacking in terthiophenes. Can J Chem 88:309-317. https://doi.org/10.1139/V09-165

[12] Zhang C, Wang X, Huang H (2008) π-Stacked interactions in explosive crystals: buffers against external mechanical stimuli. J Am Chem Soc 130:8359-8365. https://doi.org/10.1021/ja800712e

[13] Bauzá A, Sharko AV, Senchyk GA, Rusanov EB, Frontera A, Domasevitch KV (2017) π–hole interactions at work: crystal engineering with nitro-derivatives. CrystEngComm 19:1933-1937. https://doi.org/10.1039/C7CE00267J

[14] Sheldrick GM (2008) A short history of SHELX. Acta Crystallogr Sect A 64:112-122. https://doi.org/10.1107/S0108767307043930

[15] Sheldrick GM (2015) Crystal structure refinement with SHELXL. Acta Crystallogr Sect C 71:3-8. https://doi.org/10.1107/S2053229614024218

[16] Brandenburg K (1999-2022) Diamond - Crystal and Molecular Structure Visualization, Crystal Impact GbR, Kreuzherrenstr. 102, 53227 Bonn, Germany. https://www.crystalimpact.de/diamond

[17] Worrall DE (1940) Some reactions of unsaturated nitro compounds derived from terephthalaldehyde. J Am Chem Soc 62:3253-3254. https://doi.org/10.1021/ja01868a103

[18] Perekalin VV, Lerner OM (1958) The reaction of dinitrodiolefins with compounds, which contain mobile hydrogen in methylene groups. J Gen Chem USSR (Eng Trans) 28:1861-1867.

[19] Lešetický L, Flieger M, Drahorádová E (1976) Thermodynamics of *E-Z*-isomeration of β-alkyl-β-nitrostyrenes. Collect Czech Chem Commun 41:2744-2748. https://doi.org/10.1135/cccc19762744

[20] Bailey K, Legault D (1981) Analysis of the ^{13}C NMR spectra of mono and dimethoxy-β-methyl-β-nitrostyrenes: spectral assignments and conformational effests. Org Magn Reson 16:47-51. https://doi.org/10.1002/mrc.1270160113

[21] Andreev GN, Stamboliyska BA, Penchev PN (1997) Vibrational spectra and structure of 1,4-dinitrobenzene and its ^{15}N labelled derivatives: an ab initio and experimental study. Spectrochim Acta Part A 53:811-818. https://doi.org/10.1016/S1386-1425(96)01876-8

[22] R.E. Clavijo, R. Araya-Maturana, B.K. Cassels, B. Weiss-López, Infrared spectra of nitrostyrene derivatives, Spectrochim. Acta Part A 50 (1994) Pages 2105-2115. https://doi.org/10.1016/0584-8539(94)80105-3

[23] Tsuzuki S, Honda K, Uchimaru T, Mikami M (2006) Intermolecular interactions of nitrobenzene-benzene complex and nitrobenzene dimer: Significant stabilization of slipped-parallel orientation by dispersion interaction. J Chem Phys 125:124304. http://dx.doi.org/10.1063/1.2354495

[24] Tonogaki M, Kawata T, Ohba S, Iwata Y, Shibuya I (1993) Electron-density distribution in crystals of *p*-nitrobenzene derivatives. Acta Crystallogr Sect B 49:1031-1039. https://doi.org/10.1107/S0108768193005130

[25] Thalladi VR, Weiss H-C, Bläser D, Boese R, Nangia A, Desiraju GR (1998) C-H···F Interactions in the crystal structures of some fluorobenzenes. J Am Chem Soc 120:8702-8710. http://dx.doi.org/10.1021/ja981198e

[26] Boonstra EG (1963) The crystal and molecular structure of 4,4′-dinitrodiphenyl. Acta Crystallogr 16:816-823. https://doi.org/10.1107/S0365110X63002085

[27] Duschmalé J, Wennemers H (2012) Adapting to substrate challenges: peptides as catalysts for conjugate addition reactions of aldehydes to α,β-disubstituted nitroolefins. Chem Eur J 18:1111-1120. https://doi.org/10.1002/chem.201102484

[28] Daolio A, Scilabra P, Terraneo G, Resnati G (2020) C(sp^3) atoms as tetrel bond donors: A crystallographic survey. Coord Chem Rev 413:213265. https://doi.org/10.1016/j.ccr.2020.213265

[29] Loveday O, Echeverría J (2021) Methyl groups as widespread Lewis bases in noncovalent interactions. Nat Commun 12:5030. https://doi.org/10.1038/s41467-021-25314-y

[30] Spackman MA, Byrom PG (1997) A novel definition of a molecule in a crystal. Chem Phys Lett 267:215-220. https://doi.org/10.1016/S0009-2614(97)00100-0

[31] McKinnon JJ, Spackman MA, Mitchell AS (2004) Novel tools for visualizing and exploring intermol-ecular interactions in molecular crystals. Acta Crystallogr Sect B 60: 627-668. https://doi.org/10.1107/S0108768104020300

[32] Hirshfeld FL (1977) Bonded-atom fragments for describing molecular charge densities. Theor Chim Acta 44:129-138. https://doi.org/10.1007/BF00549096

[33] Spackman PR, Turner MJ, McKinnon JJ, Wolff SK, Grimwood DJ, Jayatilaka D, Spackman MA (2021) CrystalExplorer: A program for Hirshfeld surface analysis, visualization and quantitative analysis of molecular crystals. J Appl Cryst 54:1006-1011. https://doi.org/10.1107/S1600576721002910

[34] Mackenzie CF, Spackman PR, Jayatilaka D, Spackman MA (2017) CrystalExplorer model energies and energy frameworks: extension to metal coordination compounds, organic salts, solvates and open-shell systems. IUCrJ 4:575-587. https://doi.org/10.1107/S205225251700848X

[35] Konovalova IS, Shishkina SV, Bani-Khaled G, Muzyka EN, Boyko AN (2019) Intermolecular interactions in crystals of benzene and its mono- and dinitro derivatives: study from the energetic viewpoint. CrystEngComm 21:2908-2919.

https://doi.org/10.1039/C8CE02099J

[36] Xavier S, Periandy S (2015) Spectroscopic (FT-IR, FT-Raman, UV and NMR) investigation on 1-phenyl-2-nitropropene by quantum computational calculations. Spectrochim. Acta Part A 149:216-230. http://dx.doi.org/10.1016/j.saa.2015.04.055

[37] Grabowski SJ (2018) Tetrel bonds with π-electrons acting as Lewis bases - theoretical results and experimental evidences. Molecules 23:1183. https://doi.org/10.3390/molecules23051183

Index Abstract Page

High-yielding syntheses, crystal structures and Hirshfeld surface analysis of bis-1,1′-(2-nitropropenes) extended with benzene-1,4-diyl and biphenyl-4,4′-diyl spacers

Kostiantyn V. Domasevitch, Ganna A. Senchyk, Harald Krautscheid

The X-ray structures of 1,4-bis((*E*)-2-nitroprop-1-enyl)benzene and 4,4′-bis((*E*)-2-nitroprop-1-enyl)biphenyl reveal coexistence and interplay of lone pair-π-hole $NO_2\cdots NO_2$ bonds, weak hydrogen and tetrel bonds and aromatic interactions.